Biochemical and Biophysical Research Communications **280,** 68–74 (2001)
doi:10.1006/bbrc.2000.4075, available online at http://www.idealibrary.com on IDEAL®

Interaction of Antitumor Drug, Mithramycin, with Chromatin

Mohd. Ayoub Mir and Dipak Dasgupta[1]
Biophysics Division, Saha Institute of Nuclear Physics, 37 Belgachhia Road, Calcutta 700 037, India

Received November 30, 2000

Mithramycin (MTR) is an anticancer drug that blocks macromolecular biosynthesis via reversible interaction with DNA in the presence of bivalent cation such as Mg^{2+}. Mithramycin forms two types of complexes with Mg^{2+}: complex I (1:1 in terms of MTR:Mg^{2+}) and complex II (2:1 in terms of MTR:Mg^{2+}). *In vivo* antibiotic would interact with chromatin, a protein–DNA complex. For the first time we have demonstrated and characterized the association of both complexes of MTR with chromatin and nucleosome core. From an evaluation and comparison of the binding and thermodynamic parameters and CD spectra of bound complexes, we have shown the following. Histone(s) stand in the say of the access of the ligand(s) to chromosomal DNA. Chromatin and core particle interact differentially with the same ligand. Mode of interaction of the two complexes, I and II, with the same system is different. Significance of these results to understand the transcription inhibitory property of the drug in eukaryotic chromosome is discussed.

Key Words: **anticancer drug; mithramycin; chromatin; nucleosome core; mithramycin:Mg^{2+} complexes.**

Mithramycin (MTR, also known as plicamycin), from *Streptomyces plicatus,* is an anticancer antibiotic clinically employed for testicular carcinoma and Paget's disease (1). Mithramycin and other structurally related antibiotics, chromomycin A_3 and olivomycin belong to aureolic acid group of antibiotics (2). It consists of chromomycinone moiety, the aglycon ring, either side of which is linked to six member sugar residues such as D-mycarose, olivose, and oliose via *O*-glycoside linkages (2) (Fig. 1). Antitumor properties of the antibiotic in experimental tumors have been ascribed to its inhibitory role in replication and transcription process during macromolecular biosynthesis (1, 3). Prime cellular target of this antibiotic is DNA. Bivalent metal ion, such as Mg^{2+}, is an essential requirement for the (G, C) base specific association with DNA at the above neutral pH (3).

Previous studies from our laboratory have shown that in the absence of DNA, mithramycin forms two different types of complexes with Mg^{2+} depending on the concentration of Mg^{2+} (4, 5). Stoichiometries of these complexes are 1:1 (complex I) and 2:1 (complex II) in terms of drug:Mg^{2+}. These complexes are the potential DNA binding ligands at and above physiological pH. Both complexes approach the target DNA via minor grove (4–6).

DNA binding properties of this antibiotic have been well studied in our and other laboratories (4–9). *In vivo,* the antibiotic would interact with chromatin, a protein–DNA complex, in order to access the genome. It could bind via minor grove of chromatin DNA. Therefore, it is necessary to study the interaction of this drug with chromatin. In view of the role of histones in the transcriptional activity of the eukaryotic genome, we have extended our observations to examine the effect of histones upon DNA binding ability of the antibiotic in order to assess its potential as transcription inhibitor in the cell (10). So far, there is only one report that shows the binding of a related antibiotic, chromomycin with chromatin isolated from mouse and rat liver (11). This preliminary study had the following lacunae. Concentration of chromomycin used was greater than 50 μM, at which chromomycin aggregates. Mg^{2+} concentration used was in micromolar range (45–328 μM). A mixed population of complexes I and II is formed under these conditions. Knowledge about various levels of chromatin structure was also not available then. It is well established now that packaging of DNA in the eukaryotic nucleus, principal target site of the antibiotic, involves several distinct hierarchical events. First level of compaction occurs, when DNA is wrapped around an octamer of core histones to form the repeating subunit nucleosome. Histone octamer–DNA complexes are spaced at ~200 base pair intervals to form nucleosomal arrays. They interact with linker histones to form a highly folded transcriptionally suppressive "30 nm diameter chromatin fiber" (10).

[1] To whom correspondence should be addressed. Fax: +91 (33) 337 4637. E-mail: dipak@biop.saha.ernet.in.

0006-291X/01 $35.00

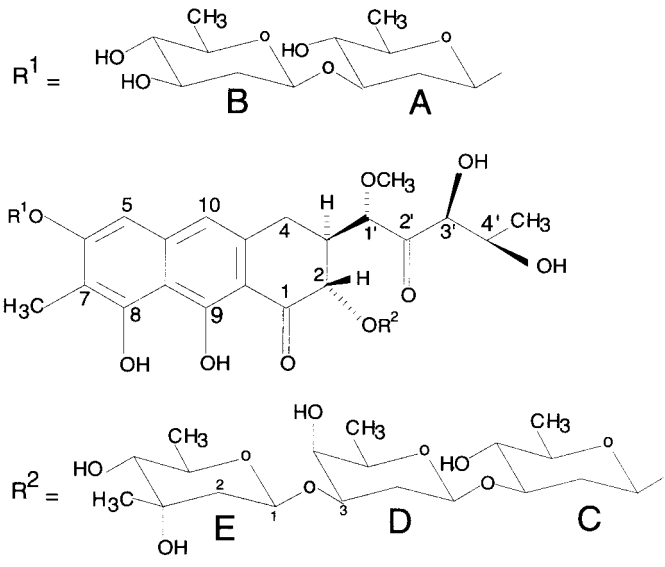

FIG. 1. Structure of mithramycin.

Work presented in this paper describes the studies on the interaction of both complexes of mithramycin with native chromatin, nucleosome core particle and DNA stripped of histone proteins from two different sources, rat and chicken liver. There are two major objectives of this study. We wanted to examine whether the distinctive nature of the two drug:Mg^{2+} complexes as DNA binding ligands (4, 6) still remains at the native chromatin or nucleosome core level. Secondly, we aimed to examine the effect of histones upon DNA binding potential of the drug:Mg^{2+} complexes at the two levels of chromatin structural organization. This is particularly relevant to understanding the mode of action of the drug in eukaryotic nucleus. In these studies, concentrations of drug and Mg^{2+} were so chosen from previous reports that they lead to the formation of a single type of complex (either complex I or complex II) (4), and we do get a mixed population of two complexes. We have found that binding parameters of rat and chicken liver chromatin at the two levels of chromatin structure follow the same trend with both complexes of mithramycin. Therefore, for detailed characterization of the association, further studies were carried with only rat liver chromatin as the representative example. The results are discussed to understand the transcription inhibitory potential of the drug.

MATERIALS AND METHODS

Mithramycin, Tris, $MgCl_2$ solution (4.9 M), $CaCl_2$ (1 M), phenyl methyl sulphonyl fluoride (PMSF), ethylene diamino tetra acetic acid, disodium salt (EDTA), Triton X-100, micrococcal nuclease and *calf thymus* DNA were from Sigma Chemical Company (USA). The buffer was prepared in quartz distilled deionized water from Milli-Q source, Millipore Corporation (USA).

Preparation of chromatin and nucleosome core particle. Male albino Sprague-Dawley rats weighing about 150 ± 10 g, about 2–3 months old, and chicken of same age, were used throughout this work. Nuclei were isolated from the homogenised liver by the standard method (12). Purified nuclei were digested with micrococcal nuclease for the preparation of chromatin (13). Prolonged digestion of nuclei with micrococcal nuclease was used to prepare the nucleosome core particle with DNA length of 147 base pairs (13, 14). Purity of the chromatin and nucleosome core particle was checked from identification of the histones in SDS–PAGE, acid urea gel, and agarose gels with appropriate markers (15). Chromatin and nucleosome core particles were estimated in terms of DNA base (16). DNA was extracted from the chromatin by repeated phenol/chloroform for quantitative estimation of base (16).

Absorbance and fluorescence measurements. Absorption and fluorescence spectra were recorded with a Hitachi U-2000 spectrophotometer and a Shimadzu RF-540 spectrofluorometer, respectively. Concentration of mithramycin was estimated from molar absorption coefficient = 10,000 M^{-1} cm^{-1} at 400 nm (6). Fluorescence excitation wavelength was 470 nm in order to avoid photodegradation of the antibiotic (6). During fluorescence measurements, absorbance of the samples did not exceed 0.05. Therefore, we did not correct the emission intensity for optical filtering effect.

Analysis of binding data. Results from fluoremetric titrations were analyzed by the following method. Apparent dissociation constant (K_d) was determined using nonlinear curve fitting analysis (Eqs. [1] and [2]). All experimental points for binding isotherms were fitted by least-square analysis (17)

$$K_d = (C_0 - (\Delta F/\Delta F_{max}) \cdot C_0) \times (C_p - (\Delta F/\Delta F_{max}) \cdot C_0)/((\Delta F/\Delta F_{max}) \cdot C_0) \quad [1]$$

$$C_0 \cdot (\Delta F/\Delta F_{max})^2 - (C_0 + C_p + K_d) \cdot (\Delta F/\Delta F_{max}) + C_p = 0. \quad [2]$$

ΔF is the change in fluorescence emission intensity at 540 nm (λ_{ex} = 470 nm) for each point of titration curve, ΔF_{max} is the same parameter when the ligand is totally bound to polymer (chromatin/nucleosome core particle/naked DNA), C_p is the concentration of the polymer (chromatin/nucleosome core particle/naked DNA), and C_0 is the initial concentration of the antibiotic. Double reciprocal plot was used for determination of ΔF_{max} using the Eq. [3]

$$1/\Delta F = 1/\Delta F_{max} + K_d/(\Delta F_{max}(C_p - C_0)). \quad [3]$$

Other details of the method are given in an earlier report.

As described in an earlier report (7) binding stoichiometry was estimated from the intersection of two straight lines of the least-square fit plot of normalized increase in fluorescence against the ratio of input concentration (in terms of DNA base) of chromatin/core particle/free DNA and drug.

Evaluation of thermodynamic parameters. Thermodynamic parameters, ΔH (Van't Hoff enthalpy), ΔS (entropy), and ΔG (free energy) were determined using the following equations (18):

$$\ln K_{app}(1/K_d) = -\Delta H/RT + \Delta S/R \quad [4]$$

$$\Delta G = \Delta H - T\Delta S \quad [5]$$

where R at T are the universal gas constant and absolute temperature, respectively. $K_{app}(1/K_d)$ was determined at three different temperatures. ΔH and ΔS were determined from the slope and intercept

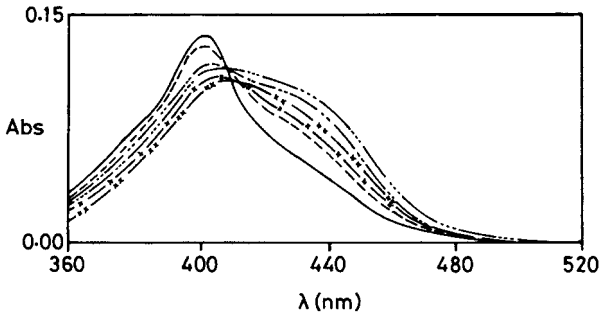

FIG. 2. Absorption spectra (360–520 nm) of MTR (13.5 μM, -) and complex I (MTR (13.5 μM) plus Mg^{2+} (230 μM)) in the absence (- - -) and presence of rat liver chromatin (340 μM, – - - –), rat liver core particle (400 μM, –x–x–), chicken liver chromatin (500 μM, – - - - –) and chicken liver core particle (500 μM, -xx-) in 10 mM Tris–HCl, pH 8.0 at 25°C.

of a plot of ln K_{app} against $1/T$. ΔG was determined from Eq. [5] after the incorporation of ΔH and ΔS values obtained from Eq. [4].

RESULTS

Change in absorption spectrum of complex I upon binding to chromatin and nucleosome core particle indicates the formation of complex between them (Fig. 2). Main feature of the change is red shift and broadening of the peak relative to that of the free antibiotic and complex I. There is a concomitant increase of the absorbance in the longer wavelength region. Similar changes were observed when complex II interact with chromatin/nucleosome core particle/naked DNA (figure not shown). These changes are characteristic of the association of the complexes with naked DNA (5, 6).

Increase in fluorescence intensity of the complexes I and II upon its association with chromatin and core particle from both sources provided us the method to evaluate the binding parameters (Figs. 3 and 4). In general, blue shift of the emission peaks accompanies the increase in fluorescence (Fig. 3). The extent of blue shift is more in case of chromatin than core particle. Increase in the quantum yield and blue shift were earlier reported for the association of the complexes with free DNA (6). Increase in fluorescence originates from a change in the local environment and/or conformation of the chromophore upon the formation of complex with chromatin/nucleosome core particle/free DNA.

We estimated the binding parameters, binding constant and stoichiometry, for the ligand–polymer interaction from fluorescence titration of a particular the ligands in presence of varying concentrations of polymer. Representative titration curves for the interaction of complex I with different systems from rat liver are shown in Fig. 4. Inset to the figure illustrates how binding stoichiometry has been determined from these results. Nature of the curves indicates a noncooperative binding between complex I and polymers over the range of input concentrations of polymer. Similar trend was observed for the interaction of complex II with the chromatin and core particle. Binding parameters were estimated similarly as described under Materials and Methods. Table 1 summarizes the binding parameters for the interaction of complexes I and II with different systems. The main points noted from the table are as follows. Presence of histone proteins in the chromatin and core particle reduces the binding affinity for both complexes, because both complexes bind to the naked DNA with comparatively higher affinity and lower stoichiometry. Among the native chromatin and core particle, the binding affinity is higher in case of the former there is a marginal increase in the binding stoichiometry in terms of covered base per drug molecule occurs from chromatin to core particle. Among the two types of complexes, affinity constant is lower for the bulkier ligand and, as expected, the binding stoichiometry is also high. Above observa-

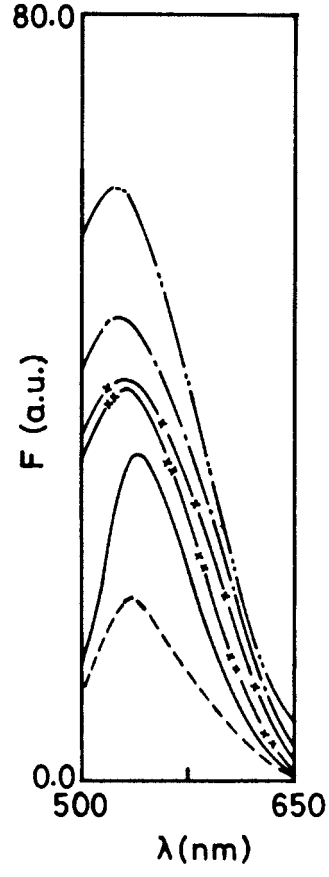

FIG. 3. Fluorescence spectra of MTR (8 μM, –) and complex I (MTR (8 μM) plus Mg^{2+} (230 μM)) in absence (- - -) and presence of rat liver chromatin (340 μM, – - –), rat liver core particle (400 μM, -xx-), chicken liver chromatin (500 μM, – - - –) and chicken liver core particle (500 μM, –x–x–) in 10 mM Tris–HCl buffer, pH 8.0 at 20°C.

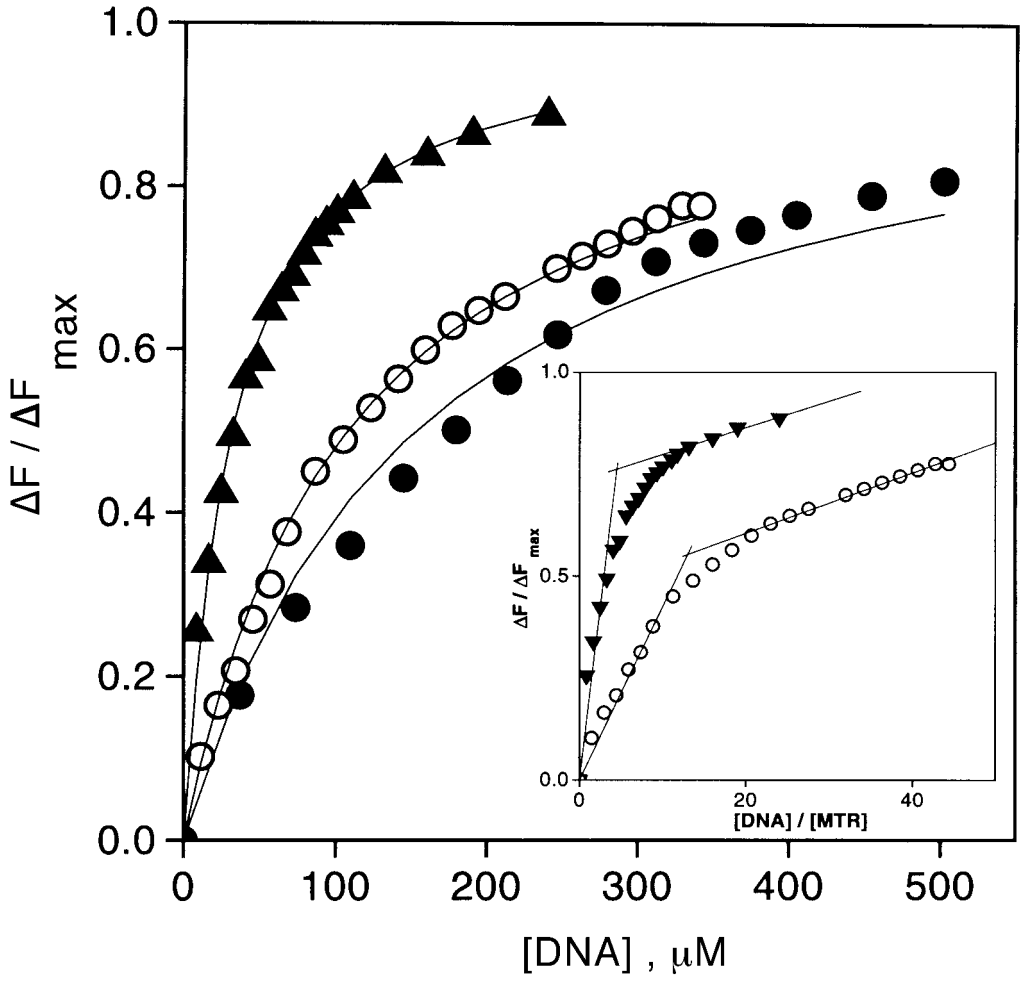

FIG. 4. Curve fitting analyses to evaluate the dissociation constant for the association of complex I with rat liver chromatin (○) and rat liver core particle (●) and dehistonized DNA (▲) in 10 mM Tris–HCl buffer, pH 8.0 at 20°C. Inset shows the determination of binding stoichiometry, for chromatin (○) and naked DNA (▲).

tions follow the same trend in two different systems, thereby justifying the generalisation of the results. Since the binding parameters follow the same trend for both rat and chicken liver chromatin, rat liver chromatin was used for the further studies.

Figure 5 shows the representative van Hoff plot for MTR II interaction with nucleosome core particle. Thermodynamic parameters for various systems are summarized in Table 2. Complex I binding is favored by enthalpy whereas complex II binding is entropy driven.

Figure 6 (a and b) shows the CD spectra of complexes I and II, respectively, in presence of saturating concentration of different polymers. The CD spectra of both the complexes of mithramycin are different in presence of native chromatin/nucleosome core particle and naked DNA. Changes in the profile and band intensity of visible CD spectra of complexes I and II occur as a result of association with DNA in the native chromatin, nucleosome. That is why the spectra of both complexes have been recorded in presence of DNA stripped of histones. In any particular set, CD spectra of the complex pass through a single point at different input concentrations of the polymer (figure not shown). Red shift of the peak in the CD spectra of both complexes upon addition of chromatin/nucleosome/naked DNA is a common feature. Spectral profiles (400–500 nm) of complex I in the presence of chromatin and naked DNA are comparable. On the other hand, spectral shape in the presence of nucleosome resembles that for free ligand. However, there is a marked reduction in the band intensities in the negative region for all cases. Situation is radically different for complex II. Differences in spectra upon addition of native chromatin, nucleosome and naked DNA are apparent.

DISCUSSION

This is the first characterization of the nature of association of the anticancer drug Mithramycin with

TABLE 1

Binding Parameters for the Interaction of MTR:Mg^{2+} Complexes with Chromatin/Nucleosome Core Particle/Free DNA in 10 mM Tris–HCl Buffer, pH 8.0 at 20°C[a]

Ligand (drug:Mg^{2+} complex)	Mg^{2+} (mM)	System	K_d[a] (μM)	n[b] (base/drug)
Rat liver				
I	0.23	Chromatin	107[c]	14 ± 2
II	2.0	Chromatin	184	33 ± 1.5
I	0.23	Core particle	154	18 ± 2
II	2.0	Core particle	201	38 ± 2.5
I	0.23	Free DNA	33	5 ± 0.5
II	2.0	Free DNA	32	7 ± 0.5
Chicken liver				
I	0.23	Chromatin	119	15
II	2.0	Chromatin	134	29
I	0.23	Core particle	163	19
II	2.0	Core particle	187	42
I	0.23	Free DNA	23	6
II	2.0	Free DNA	25	8

[a] The values of apparent dissociation constant were obtained by nonlinear curve fit method as described under Materials and Methods.
[b] Binding stoichiometry expressed in terms of site size was calculated from the titration profile using the method described in Ref. 20.
[c] The standard deviation from three sets of experiment is 15%.

different levels of chromatin structure. The DNA binding property of this drug and the related antibiotic, chromomycin in chromatin is well known because they are widely used as chromosomal staining agent in karyotyping. Two major conclusions from our report are as follows.

First, presence of associated histone proteins in chromatin and nucleosome core particle has a negative effect upon DNA-binding potential of both complexes of mithramycin. The effect is more pronounced with the bulkier complex II. Same trends in the results from both rat liver and chicken liver reinforce the conclusion. The negative effect is anticipated considering the reported crystal structure of nucleosome (19). Some of the minor grooves of DNA in the nucleosome are occupied by the arginine side chains of histone.

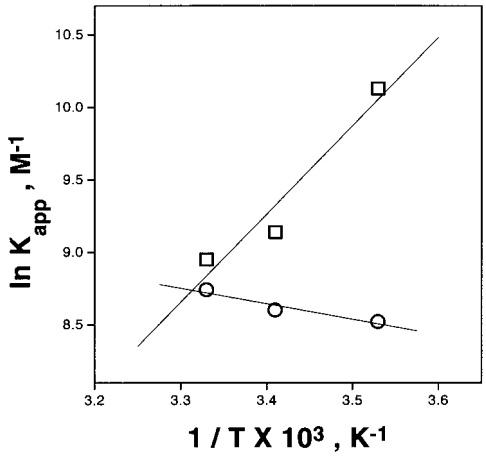

FIG. 5. van Hoff plots for the interaction of complex I (□) and complex II (○) with native chromatin in 10 mM Tris–HCl buffer, pH 8.0.

TABLE 2

Thermodynamic Parameters for the Interaction of Complex I and II of Mithramycin with Rat Liver Native Chromatin, Nucleosome Core Particle, and Naked DNA in 10 mM Tris–HCl, pH 8.0 at 25°C

System	ΔG (Kcal/mol)	ΔH (Kcal/mol)	ΔS (e.u)
	Complex I		
Native chromatin	−5.3	−12.0	−22.6
Nucleosome core particle	−5.0	−9.8	−16.0
Naked DNA	−5.9	−7.5	−5.5
	Complex II		
Native chromatin	−5.1	2.1	24.3
Nucleosome core particle	−5.1	4.6	32.6
Naked DNA	−6.1	3.5	32.3

Secondly, difference in the binding potential and binding stoichiometry of complexes I and II further supports our proposition that these complexes are different molecular species with distinctive three dimensional structures. Since *in vivo* concentration of Mg^{2+} is high (10 mM), chances of formation of complex II is greater. However, formation of complex I can not be ruled out under certain special conditions. There are reported fluctuations in the Mg^{2+} concentrations in carcinogenic tissues (20). Each of these aspects is discussed below.

Neither of the two ligands bind to any histone. Independent experiments using fluorescence property of the drug have shown the absence of such interactions (not shown). In view of this observation and the earlier well-established documentation of the ligand(s)–DNA interaction, present result suggests that histone–DNA contacts in chromatin and nucleosome core particle reduce the accessibility of minor groove of (G, C) rich region of chromosomal DNA to both complexes of mithramycin. Among native chromatin and nucleosome core particle, we notice a small but consistent reduction in binding affinity and increase in site size upon removal of linker DNA in nucleosome. Analysis of the CD spectral features of bound complexes also suggest that the environments of the chromophore in both ligands are different in chromatin and core particle. These features may be ascribed to a loss of binding site in linker DNA as we go from chromatin to nucleosome.

The aforementioned results have another biological significance. During eukaryotic transcription, Histone H1 undergoes covalent modification that leads to its dissociation from the DNA. During histone H1 depletion nearly 20 base pairs of DNA leave the histone

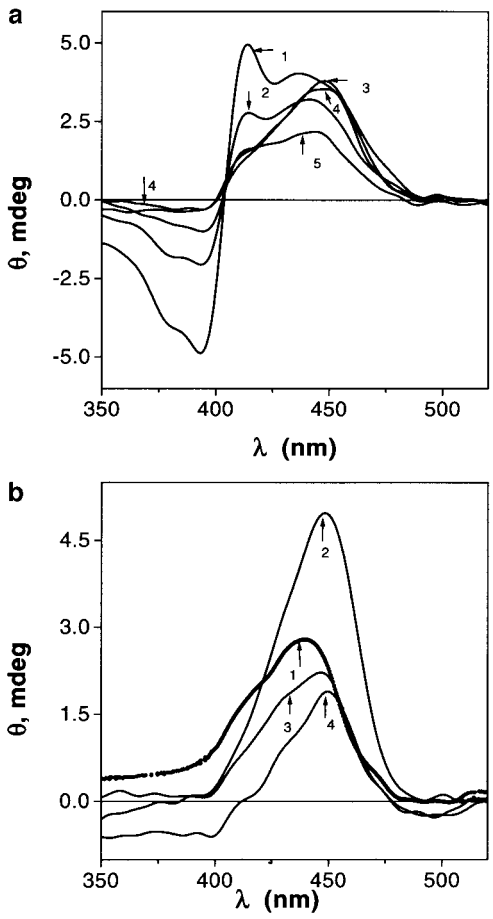

FIG. 6. CD spectra (350–520 nm) of complexes I and II under different conditions in 10 mM Tris–HCl buffer, pH 8.0 at 25°C. (a) MTR (15 μM) alone (1), complex I (MTR (15 μM) plus Mg^{2+} (230 μM)) (2), complex I in presence of 132 μM of rat liver naked DNA (3), complex I in presence of 340 μM of rat liver native chromatin (4), and complex I in presence of 400 μM of rat liver core particle (5). (b) Complex II (MTR (15 μM) plus Mg^{2+} (2 mM)) (1), complex II in presence of 132 μM of rat liver naked DNA (2), complex II in presence of 804 μM of rat liver core particle (3), and complex II in presence of 736 μM of rat liver native chromatin (4).

contact and are exposed (21, 22). The pattern of micrococcal nuclease digestion within a domain, reflecting chromosome structure at the level of the nucleosomes, is not much affected by the transcription, except at sequences such as enhancers and promoters. They become "hypersensitive" to digestion, due to the loss of nucleosomes (23, 24), thus providing the naked DNA regions due to histone loss. The higher affinity of both the complexes of mithramycin, which are transcription inhibitors, for dehistonized DNA can be appreciated from this perspective.

REFERENCES

1. Calabresi, P., and Chabner, B. A. (1991) *in* The Pharmacological Basis of Therapeutics (Goodman and Gilmann, Eds.), pp. 1209–1263, Macmillan, NY.
2. Wohlert, S. E., Kunzel, E., Machinek, R., Mendez, C., Salas, and Rohr, J. A. (1999) The structure of Mithramycin reinvestigated. *J. Nat. Prod.* **62,** 119–121.
3. Goldberg, I. H., and Friedmann, P. A. (1971) Antibiotics and nucleic acids. *Annu. Rev. Biochem.* **40,** 775–779.
4. Aich, P., and Dasgupta, D. (1990) Role of Mg^{2+} in the Mithramycin–DNA interaction: Evidence for the two types of Mithramycin–Mg^{2+} complexes. *Biochem. Biophys. Res. Commun.* **14,** 689–696.
5. Aich, P., Sen, R., and Dasgupta, D. (1992) Role of Magnesium ion in the interaction between Chromomycin A_3 and DNA: Binding of Chromomycin A_3-Mg^{2+} complexes with DNA. *Biochemistry* **31,** 2988–2997.
6. Aich, P., and Dasgupta, D. (1995) Role of magnesium ion in the Interaction between Mithramycin and DNA—Binding of Mithramycin-Mg(II) complexes with DNA, *Biochemistry* **34,** 1376–1385.
7. Majee, S., Sen, R., Guha, S., Bhattacharya, D., and Dasgupta, D. (1997) Differential interaction of the Mg^{2+} complexes of Chromomycin A_3 and Mithramycin with poly(dG-dC) · poly(dC-dG) and poly(dG) · poly(dC). *Biochemistry* **36,** 2291–2299.
8. Keniry, M. A., Banville, D. L., Simmonds, P. M., and Shafer, R. H. (1993) Nuclear magnetic resonance comparison of the binding sites of mithramycin and chromomycin on the self-complementary oligonucleotide $d(ACCCGGGT)_2$. Evidence that the saccharide chains have a role in sequence specificity. *J. Mol. Biol.* **231,** 753–767.
9. Sastry, M., Fiala, R., and Patel, D. J. (1995) Solution structure of mithramycin dimers bound to partially overlapping sites on DNA. *J. Mol. Biol.* **251,** 674–689.
10. Kornberg, R. D., and Lorch, V. (1999) Twenty-five years of the nucleosome, fundamental particle of the eukaryotic chromosome. *Cell* 285–299.
11. Nayak, R., Sirsi, M., and Podder, S. K. (1975) Mode of action of antitumor antibiotics Spectrophotometric studies on the interaction of Chromomycin A_3 with DNA and chromatin of normal and neoplastic tissue. *Biochim. Biophys. Acta* **378,** 195–208.
12. Blobel, G., and Potter, V. R. (1966) Nuclei from rat liver: Isolation method that combines purity with high yield. *Science* **154,** 1662–1665.
13. Kornberg, R. D., Lapointe, J. W., and Yahlilorch. Preparation of nucleosomes and chromatin. *Methods Cell Biol.* **170,** 3–25.
14. Rao, M. R. S., Rao, B. J., and Ganguly, J. (1982) Localization of testis-variant histones in rat testis chromatin. *Biochem. J.* **20,** 15–21.
15. Panyim, S., and Chalkley, R. (1969) High resolution acrylamide gel electrophorses of histones. *Arch. Biochem. Biophys.* **130,** 337–346, 69–103.
16. Burton, K. (1956) A study of the conditions and mechanism of the diphenylamine reaction for the colorimetric estimation of deoxyribonucleic acid. *Biochem. J.* **62,** 315–323.
17. Chakrabarty, S., Roy, P., and Dasgupta, D. (1998) Interaction of the antitumor antibiotic, Chromomycin A3, with sulfhydryl agent, glutathione, and the effect upon its DNA binding properties. *Biochem. Pharmacol.* **56,** 1471–1479.
18. Castellan, G. W. (1989) *in* Physical Chemistry 3rd ed., p. 799, Addison Wesley/Narosa Publishing House, New Delhi, India.
19. Luger, K., Mader, A. W., Richmond, R. K., Sargent, D. F., and Richmond, T. (1997) Crystal structure of the nucleosome core particle at 2.8A resolution. *Nature* **389,** 251–260.
20. Sigel, H., and Sigelds, A. (1990) Metal ions in biological system (Compendium on magnesium and its role in biology, nutrition, and physiology), New York-Basel. **26,** 243–247.
21. Noll, M., and Koreberg, R. D. (1977) Action of micrococcal nucle-

ase on chromatin and the location of H1. *J. Mol. Biol.* **109,** 393–404.

22. Varshavsky, A., Sundin, O., and Bohn, M. (1979) A stretch of "late" SV40 viral DNA about 400 bp long which includes the origin of replication is specifically exposed in SV40 minichromosomes. *Cell* **16,** 453–466.
23. Wu, C. (1980) The 5′ ends of Drosophila heat shock genes in chromatin are hypersensitive to DNase 1. *Nature* **286,** 854–860.
24. Almer, A., and Horz, W. (1986) Nuclease hypersensitive regions with adjacent positioned nucleosomes mark the gene boundaries of the PHO5/PHO3 locus in yeast. *EMBO J.* **5,** 2681–2687.